bioRxiv preprint doi: https://doi.org/10.1101/156232; this version posted June 26, 2017. The copyright holder for this preprint (which was not certified by peer review) is the author/funder, who has granted bioRxiv a license to display the preprint in perpetuity. It is made available under aCC-BY-NC-ND 4.0 International license.

1 # Title page

2 **Classification:** Biological sciences, Genetics

3 **Title:** Characterization of SID-1-dependent and independent intergenerational RNA
4 transport pathways in *Caenorhabditis elegans*

5 **Authors:** Eddie Wang[1], Craig P. Hunter[1]

6 **Author affiliation:** [1]Department of Molecular and Cellular Biology, Harvard University,
7 Cambridge, MA 02138

8 **Corresponding author:** Craig P. Hunter, 16 Divinity Avenue Room 3044, Cambridge,
9 MA 02138. (617)495-8305. hunter@mcb.harvard.edu

10 **Keywords:** *Caenorhabditis elegans*, RNAi, double-stranded RNA, yolk

bioRxiv preprint doi: https://doi.org/10.1101/156232; this version posted June 26, 2017. The copyright holder for this preprint (which was not certified by peer review) is the author/funder, who has granted bioRxiv a license to display the preprint in perpetuity. It is made available under aCC-BY-NC-ND 4.0 International license.

Abstract

Systemic RNA interference (RNAi) in *C. elegans* is dependent on *sid-1* (WINSTON *et al.* 2002), *sid-3* (JOSE *et al.* 2012) and *sid-5* (HINAS *et al.* 2012). After injection, expression, or ingestion, double-stranded RNA (dsRNA) is transported between cells throughout the animal to enable RNAi in most tissues, including the germline and progeny. Here, we characterize the role of the Sid genes in transport of dsRNA to progeny. We previously reported that dsRNA injected directly in the germline unexpectedly requires *sid-1* activity in the progeny to initiate RNAi (WINSTON *et al.* 2002). We now show that germline injected dsRNA can travel by three independent pathways to silence gene expression in embryos. First, germline injected dsRNA is delivered, presumably by bulk flow, into oocytes and embryos. This means of delivery, which does not require *sid-1,* is limited by the amount and location of injected dsRNA. Second, maternal *sid-1* transports extracellular dsRNA into the germline where it can silence maternal deposited mRNAs and segregate to embryos to silence embryonically expressed mRNAs. Third, extracellular dsRNA is also endocytosed into oocytes by the low-density lipoprotein (LDL) receptor superfamily homolog RME-2. The endocytosed dsRNA then requires *sid-1* and *sid-5* in embryos to silence embryonically expressed genes. Extracellular fluorescent dsRNA, once endocytosed into oocytes, does not co-localize with VIT-2::GFP and it does not require *sid-1* activity to segregate from the late endocytosis marker GFP::RAB-7 in early embryos. In conclusion, we identify genes and pathways that function redundantly for intergenerational RNA transfer that may represent mechanisms for transgenerational epigenetic inheritance.

Introduction

RNA interference is a powerful and well-conserved mechanism for sequence specific gene silencing (HUTVÁGNER AND ZAMORE 2002). Introduced double stranded RNA (dsRNA) triggers degradation of homologous transcripts (FIRE *et al.* 1998; HAMILTON AND BAULCOMBE 1999; ZAMORE *et al.* 2000; SHARP 2001) as well as subsequent transcriptional gene silencing (GUANG *et al.* 2008; GUANG *et al.* 2010; BUCKLEY *et al.* 2012). In some animals including the nematode *C. elegans*, RNAi is systemic; dsRNA introduced into the animal by any of several methods results in rapid spread of silencing throughout the animal (FIRE *et al.* 1998; IVASHUTA *et al.* 2015). This systemic silencing requires the dsRNA channel SID-1, which imports dsRNA into the cytoplasm (WINSTON *et al.* 2002; FEINBERG AND HUNTER 2003; SHIH AND HUNTER 2011). SID-1 supports particularly effective silencing in the progeny of dsRNA exposed mothers (FIRE *et al.* 1998; GRISHOK *et al.* 2000; ALCAZAR *et al.* 2008), implying transfer of dsRNA from mother to embryo.

SID-1 dependent heritable RNAi can be initiated by ingesting dsRNA expressing bacteria, by tissue-specific expression of dsRNA from transgenes , and by dsRNA injection into somatic tissues, the germline, or the pseudocoelom (PC, body cavity) (JOSE *et al.* 2009). Initial investigation of *sid-1*-dependent heritable RNAi by dsRNA injection showed that dsRNA targeting a germline expressed mRNA injected into the gonad of *sid-1* mutant animals produced affected progeny, while injection into the intestine or the PC produced no affected progeny (WINSTON 2002; WINSTON *et al.* 2002).

bioRxiv preprint doi: https://doi.org/10.1101/156232; this version posted June 26, 2017. The copyright holder for this preprint (which was not certified by peer review) is the author/funder, who has granted bioRxiv a license to display the preprint in perpetuity. It is made available under aCC-BY-NC-ND 4.0 International license.

56 Similar injections into wild-type animals produced near 100% affected progeny. These
57 results showed that *sid-1* is required for transport of dsRNA into the germline, but is not
58 required for RNAi itself in the germline. Similar results were expected for injection of
59 dsRNA targeting the somatic muscle gene *unc-22*, which is required for normal muscle
60 function. However, while *unc-22* dsRNA injection into wild-type animals produced many
61 affected progeny, similar injections into *sid-1* mutants failed to produce affected progeny,
62 even among the progeny of germline injected mothers. This was unexpected because
63 the syncytial germline cytoplasm is continuous with the oocyte/embryo cytoplasm and
64 thus SID-1 should not be required. Also unexpectedly, crossing wild-type males to *unc-*
65 *22* dsRNA injected *sid-1* mutant hermaphrodites restored silencing to the progeny. This
66 was true for both germline injected mothers (WINSTON *et al.* 2002) as well as PC
67 injected mothers (WINSTON 2002). These results revealed a role for *sid-1* in the embryo
68 and an unidentified *sid-1*-independent pathway for dsRNA transport to embryos.
69 Here we report a detailed genetic and cytological investigation of dsRNA
70 transport into oocytes and embryos. We identify three dsRNA transport process that
71 support inherited RNAi. First, as expected, germline injected dsRNA segregates,
72 independent of *sid-1* activity, to embryos resulting in temporally limited silencing.
73 Second, maternally expressed *sid-1* transports extracellular dsRNA into the germline.
74 Third, the LDL receptor superfamily homolog RME-2 enables endocytosis of dsRNA into
75 oocytes, but to initiate RNAi in the resulting embryos zygotic *sid-1* and *sid-5* are
76 required, presumably to release membrane encapsulated dsRNA into the cytosol. Marré
77 *et al.* recently confirmed the published observations (WINSTON 2002; WINSTON *et al.*
78 2002) on an embryonic role for *sid-1* and the presence of a *sid-1*-independent transport
79 process and also identified RME-2 as important for this *sid-1* independent dsRNA
80 transport (MARRÉ *et al.* 2016). In contrast to Marré *et al.*, our analysis shows that
81 maternal RME-2 and SID-1 act independently, as neither single mutant prevents dsRNA
82 transport to embryos. Our analysis of this discrepancy revealed a strong effect of
83 maternal developmental stage on inherited RNAi, which only strengthens the
84 discrepancy. Our analysis of injected labeled dsRNA shows that although dsRNA and
85 the yolk marker VIT-2::GFP co-localize in the PC space and even on the surface of the
86 oocyte, internalized VIT-2::GFP and dsRNA do not co-localize. Furthermore, labeling
87 dsRNA with Cy5 interferes with dsRNA transport into oocytes. This indicates that non-
88 specific interactions between yolk and dsRNA are unlikely to account for the RME-2
89 mediated uptake. Our genetic analysis of post-endocytosis dsRNA trafficking shows that
90 dsRNA either exits the endocytosis pathway early or rapidly transits the pathway
91 independently of *sid-1*, as dsRNA and late endosome markers do not significantly co-
92 localize in either wild-type or *sid-1* mutant embryos.
93

bioRxiv preprint doi: https://doi.org/10.1101/156232; this version posted June 26, 2017. The copyright holder for this preprint (which was not certified by peer review) is the author/funder, who has granted bioRxiv a license to display the preprint in perpetuity. It is made available under aCC-BY-NC-ND 4.0 International license.

94 # Results
95 ## Inherited silencing in the absence of *sid-1*
96 SID-1 is required to transport dsRNA or derived silencing signals to the germline, as
97 shown by injecting dsRNA into specific tissues or the PC (WINSTON 2002; WINSTON *et al.*
98 2002). However, while *unc-22* dsRNA injection into any tissue in wild-type animals
99 resulted in silenced progeny, *unc-22* dsRNA injected into the syncytial germline of a *sid-*
100 *1* mutant, unexpectedly, did not result in any affected progeny (WINSTON 2002; WINSTON
101 *et al.* 2002). To further investigate this result, we injected *unc-22* dsRNA directly into the
102 syncytial gonads of wild-type and *sid-1* mutant adult hermaphrodites and every two
103 hours after injection collected their self-progeny. As expected, and consistent with
104 previous observations of systemic silencing, the proportion of twitching progeny from
105 injected wild-type animals quickly rose to 100% and was sustained for the duration of
106 the experiment (Fig. 1*B*). In contrast to previous observations, we found that injecting
107 dsRNA directly into the syncytial gonads of *sid-1*$^{-/-}$ animals produced strongly twitching
108 progeny. However, this was only true of embryos laid within approximately the first 18
109 hours after injection (Fig. 1*A*). The timing of peak silencing varied between injected P_0
110 animals, but always reached 100% (Fig. *S*1). The subsequent decrease in fraction of
111 silenced F_1 embryos to zero suggests that the injected *unc-22* dsRNA is rapidly
112 depleted. In the previous experiments (WINSTON 2002; WINSTON *et al.* 2002), the
113 injected hermaphrodites were allowed to recover for up to 24 hours before progeny
114 were collected and scored for silencing. The apparent rapid depletion of syncytial
115 germline injected dsRNA explains the past failure to detect *sid-1*-independent silencing.
116 Furthermore, when a single gonad arm was injected in *sid-1* mutant animals, only a
117 maximum of 50% twitching progeny was produced (Fig. 1*C*, *S*1). Thus, *sid-1*
118 independent silencing is restricted to the cytoplasm containing the injected dsRNA. In
119 contrast, the control injections into a single gonad of wild-type hermaphrodites clearly
120 show gonad injected dsRNA is mobile between gonad arms (Fig. 1*D*). Additionally, in
121 wild type animals, dsRNA or a derived silencing signal persists indefinitely in the
122 injected hermaphrodites. Interestingly, injecting *unc-22* dsRNA into a single gonad arm
123 of *sid-1* mutant hermaphrodites and then crossing them to wild-type males produced
124 nearly 100% affected heterozygous cross progeny (Fig 1*E*). This indicates that *sid-1*
125 activity in the mother is not required for either gonad to gonad transfer of dsRNA or the
126 long-term persistence of the silencing signal, and that *sid-1* activity in the embryo is
127 required to access this dsRNA or derived silencing signal.
128
129 ## *sid-1*-independent dsRNA Transmission Requires RME-2
130 The above results, showing *sid-1*-independent delivery of dsRNA from mothers to
131 embryos and a *sid-1*-dependent step in the embryos for effective RNAi is similar to
132 feeding RNAi, where the uptake and transport of ingested dsRNA is separable. Feeding
133 RNAi first requires SID-2, an intestinal-lumen-localized transmembrane protein, for
134 endocytosis of ingested dsRNA, and SID-1 is required subsequently for effective RNAi
135 within intestinal cells, likely to release dsRNA from endosomes (WINSTON *et al.* 2007;
136 MCEWAN *et al.* 2012). A candidate receptor for similar dsRNA endocytosis in the
137 germline is RME-2, an LDL receptor superfamily homolog that functions in oocytes as a
138 yolk/lipoprotein receptor. In *C. elegans,* yolk is synthesized in the intestine, exported to
139 the PC, and then taken up by oocytes via receptor-mediated endocytosis (SHARROCK *et*

bioRxiv preprint doi: https://doi.org/10.1101/156232; this version posted June 26, 2017. The copyright holder for this preprint (which was not certified by peer review) is the author/funder, who has granted bioRxiv a license to display the preprint in perpetuity. It is made available under aCC-BY-NC-ND 4.0 International license.

140 *al.* 1990; GRANT AND HIRSH 1999). Thus, we hypothesized that PC dsRNA may bind to
141 either yolk protein, another RME-2 substrate, or directly to RME-2 for endocytosis into
142 oocytes. To test this hypothesis, we examined *rme-2*$^{-/-}$ mutants, which do not take up
143 any yolk (GRANT AND HIRSH 1999) We injected *unc-22* dsRNA into the PC of *rme-2*$^{-/-}$*;*
144 *sid-1*$^{-/-}$ double mutant hermaphrodites and then crossed these animals to wild-type
145 males. The heterozygous cross progeny did not twitch, showing that RME-2 is required
146 for heritable RNAi (Fig. 3A). This indicates that RME-2 can endocytose PC dsRNA into
147 oocytes. Similar findings were recently reported by Marré *et al.* (MARRÉ *et al.* 2016).
148
149 **SID-1 is sufficient in the germline to transmit maternal dsRNA to progeny**
150 SID-1 and SID-2 are both individually required for feeding RNAi (WINSTON *et al.* 2007).
151 That is, SID-1 is not sufficient to transport ingested dsRNA into intestinal cells. To
152 determine whether RME-2 and SID-1 must similarly function together to deliver PC
153 dsRNA to the silencing components in embryos we injected *unc-22* dsRNA into the PC
154 of *rme-2*$^{-/-}$single mutants. We found that their progeny showed Unc-22 defects (Fig. 3*A*).
155 This result indicates that, unlike the case in the intestine, SID-1 may directly transport
156 PC dsRNA to oocytes and embryos.
157 This finding contrast with recent results reporting that *rme-2* single mutants were
158 defective for inherited RNAi initiated by consuming *unc-22* dsRNA (MARRÉ *et al.* 2016).
159 The difference in potency between feeding RNAi used by Marré *et al.,* and PC injection
160 of concentrated *in vitro* transcribed dsRNA as described above may explain their
161 negative result. To address this, we attempted to repeat their feeding RNAi assay as
162 described, *i.e.* exposing L4 hermaphrodites to *unc-22* dsRNA-expressing bacteria for
163 one day before washing and transferring to control bacteria. By these methods, we
164 failed to detect robust inherited RNAi among the progeny of wild-type parents. Further
165 analysis revealed a striking dependency on maternal developmental stage for inherited
166 silencing. We split a batch of freshly hatched wild-type larvae into 3 populations and
167 exposed each to *unc*-22 RNAi food on either day 1 (L1/L2), day 2 (L3/L4), or day 3
168 (adult) after hatching, thoroughly washing off residual bacteria each day. After a final
169 wash, animals were allowed to lay F_1 progeny on non-RNAi food. We found that only
170 animals exposed to *unc-22* food as adults efficiently produced twitching progeny (Fig.
171 3B), even though the P_0 animals fed on days 1 and 2 still exhibited a strong Unc-22
172 twitching phenotype immediately after RNAi exposure. Using these conditions, we found
173 that the progeny of wild type and *rme-2* adults placed on *unc-22* food show similar
174 proportions of twitching progeny (Fig. 3C). Similarly, *rme-2* L4 animals exposed to RNAi
175 do not produce twitching progeny, in agreement with Marré *et al*. Because inherited
176 RNAi by dsRNA feeding requires adult exposure, it is reasonable to assume that the
177 slightly slower development of *rme-2* mutants differentially limited the period of adult
178 exposure compared to wild-type animals when initially placed on the RNAi food as L4
179 larvae. In conclusion, independent of the means of dsRNA delivery, *rme-2* is not
180 required for transport of dsRNA into the germline.
181
182 ***sid-5* functions with *sid-1* in the embryo**
183 Pseudocoelomic *unc-22* dsRNA transported into oocytes or embryos in the absence of
184 maternal *sid-1* requires embryonic *sid-1* to silence *unc-22*. We next asked whether *sid-2*,
185 *sid-3*, or *sid-5* are also required in the embryo. We first crossed *sid-1; sid-2* double

bioRxiv preprint doi: https://doi.org/10.1101/156232; this version posted June 26, 2017. The copyright holder for this preprint (which was not certified by peer review) is the author/funder, who has granted bioRxiv a license to display the preprint in perpetuity. It is made available under aCC-BY-NC-ND 4.0 International license.

186 mutant hermaphrodites injected with *unc-22* dsRNA to either wild type or *sid-2* males
187 and scored silencing in the cross progeny. If *sid-2* activity is required in the embryo,
188 then the cross progeny of only the wild type males will twitch. If *sid-2* activity is not
189 required in the embryo, then the cross progeny of both wild type and *sid-2* males will
190 twitch. Using this method we determined that neither *sid-2* nor *sid-3* are required for
191 either maternal uptake or embryonic release (Fig. 2A,B), but we found a striking
192 requirement for *sid-5* for embryonic release.
193 SID-5 is an endosome-associated protein required for efficient systemic RNAi
194 (HINAS *et al.* 2012). In our double mutant rescue experiments, no silencing was
195 observed in the next generation if *sid-5* is not rescued (Fig. 2*C*), the same effect as if
196 *sid-1* is not rescued. Because *sid-5* is located on the X-chromosome, crossing a *sid-1*$^{-/-}$*;*
197 *sid-5*$^{-/-}$ hermaphrodite to a wild-type male results in heterozygous *sid-5*$^{+/-}$ hermaphrodite
198 progeny and hemizygous *sid-5*$^{0/-}$ mutant male progeny. When performing the *unc-22*
199 dsRNA PC injection and rescue in this context, we saw that 100% of hermaphrodite
200 progeny but none of the male progeny showed the *unc-22* silencing phenotype (Fig. 2*C*).
201 The importance of SID-5 in the context of *sid-1*-independent transmission of RNA is
202 especially surprising given the previous reports of only weak systemic RNAi defects for
203 *sid-5* mutants (HINAS *et al.* 2012). However, those experiments were performed in the
204 context of fully functional and normally expressed SID-1, in which case there may be
205 alternative routes for RNA to reach the cytoplasm that are less dependent on SID-5.
206
207 **Labeled Nucleotides Can Be Used to Visualize Functional Transported dsRNA**
208 Our finding that RME-2 is required for silencing signals to reach developing oocytes and
209 embryos suggests an association between RNA and yolk. We sought evidence of this
210 association by labeling and visualizing both components. We synthesized *unc-22*
211 dsRNA using 5-ethynyluridine (5EU) nucleotides, replacing a significant fraction of the
212 normal uridine nucleotides with nucleotides carrying the modified base. 5EU carries a
213 small alkyne modification that allows the RNA to be easily visualized after fixation and
214 labeling through click chemistry (JAO AND SALIC 2008). 5EU-labeled *unc-22* dsRNA
215 injected into a single gonad arm of a wild-type worm results in >50% twitching progeny,
216 indicating that, like unmodified dsRNAs, 5EU dsRNA is both mobile and capable of
217 silencing target genes (Fig 4*A*).
218 To determine whether fluorescently labeled 5EU signal represents intact dsRNA
219 and not degraded nucleotides or other irrelevant species, we used a second label and
220 synthesized dsRNA composed of one strand labeled with 5EU and the other strand
221 internally labeled with Cy5-uridine. Although Cy5-labeled dsRNA is not capable of
222 systemic RNAi, it suffices for demonstrating the properties of labeled dsRNA. We
223 injected the Cy5:5EU duplex dsRNA into the PC of adult hermaphrodites and several
224 hours later fixed the animals to visualize both labels (Fig. 4*B*). Much of the signal
225 appears in the pseudocoelom as pools surrounding other tissues. Importantly, both
226 labels are detected in the same locations and their intensities appear closely correlated.
227 Coinciding labeled RNA was also detected in punctate foci in coelomocytes, providing
228 further evidence for the structure and stability of the injected RNA.
229 In addition to the Cy5:5EU duplex, we also injected a 1:1 mixture of Cy5-labeled
230 dsRNA with 5EU-labeled dsRNA. We found that although these mixed dsRNAs were
231 both readily detectable in the PC, their apparent relative abundances were much less

bioRxiv preprint doi: https://doi.org/10.1101/156232; this version posted June 26, 2017. The copyright holder for this preprint (which was not certified by peer review) is the author/funder, who has granted bioRxiv a license to display the preprint in perpetuity. It is made available under aCC-BY-NC-ND 4.0 International license.

232 well-correlated than the co-labeled duplex dsRNA, and more frequently one label could
233 be seen without the other (Fig. 4*C*). That is, when not physically bound together, each
234 label appears free to vary independently. Together, these data suggest that 5EU
235 fluorescence represents *bona fide* dsRNA as opposed to disassociated strands or
236 degraded nucleotides or labels.
237 We also attempted to detect labeled RNA in embryos from PC-injected
238 hermaphrodites. The Cy5:5EU heteroduplex was not detected above background in
239 embryos (Fig. 4*D*). Furthermore, while we could detect 5EU-labeled RNA punctae in
240 embryos, the co-injected Cy5-labeled RNA was only detected in the PC and
241 coelomocytes (Fig. 4*E*). These observations are consistent with Cy5-containing RNA
242 being impaired for normal trafficking while 5EU-labeled RNA behaves as expected for
243 unmodified RNA. The inability of either the Cy5:5EU heteroduplex or Cy5-RNA to enter
244 embryos suggests there is selectivity in the RME-2-dependent transmission process.
245 Such selectivity is not expected if dsRNA is simply hitchhiking on yolk proteins.
246
247 **Labeled dsRNA and VIT-2::GFP largely fail to co-localize**
248 We next sought to characterize the relationship between dsRNA and yolk. Previous
249 studies have shown co-localization of yolk and end-labeled dsRNA that lessens after
250 fertilization (MARRÉ *et al.* 2016). We injected our 5EU-labeled dsRNA into the PC of
251 adults expressing GFP-labeled yolk (*vit-2::GFP*) and imaged the injected adults as well
252 as isolated embryos. We detected 5EU-labeled dsRNA co-localized with VIT-2::GFP
253 granules at the surface of developing oocytes in adult gonads (Fig. 5*A*), in agreement
254 with prior observations (MARRÉ *et al.* 2016). This co-localization is consistent with co-
255 dependence on oocyte-expressed RME-2 for the uptake of yolk and RNA. However,
256 interior sections contain 5EU punctae not associated with any yolk, suggesting that
257 although they may share the same endocytosis receptor, they are either separately
258 endocytosed or sorted to different endosomes soon after import. While previous studies
259 reported loss of co-localization in embryos past the 4-cell stage (MARRÉ *et al.* 2016),
260 higher resolution imaging suggests that the separation of yolk and dsRNA can be seen
261 even earlier in oocytes soon after import (Fig. 5*A*). Analysis of 5EU-labeled dsRNA and
262 VIT-2::GFP in embryos is consistent with this view. The majority of detectable 5EU
263 fluorescence in embryos does not co-localize with GFP fluorescence (Fig. 5*B*). The lack
264 of co-localization might reflect *sid-1*-dependent release of dsRNA from endosomes.
265 However, in *sid-1*$^{-/-}$ mutant embryos labeled dsRNA also fails to co-localize with VIT-
266 2::GFP (Fig. 5*B*). This further supports the idea that although dsRNA and yolk share a
267 common mechanism for endocytosis into oocytes, they likely do not share common
268 endosomal compartments.
269
270 **dsRNA Transits RAB-7-Containing Vesicles Independent of SID-1**
271 Since internalized dsRNA appears to be physically separate from yolk granules, we
272 wondered whether the 5EU punctae might co-localize with the late endosome marker
273 RAB-7 (FENG *et al.* 1995; GRANT AND HIRSH 1999). We injected adult hermaphrodites in
274 the PC with 5EU-labeled dsRNA and visualized the resulting embryos in conjunction
275 with antibody staining against GFP-labeled RAB-7. In wild-type embryos, we
276 occasionally detected dsRNA together with RAB-7-positive vesicles, but the majority of
277 the 5EU punctae were not associated with GFP-RAB-7 (Fig. 6*A*, upper row). In *sid-1*

bioRxiv preprint doi: https://doi.org/10.1101/156232; this version posted June 26, 2017. The copyright holder for this preprint (which was not certified by peer review) is the author/funder, who has granted bioRxiv a license to display the preprint in perpetuity. It is made available under aCC-BY-NC-ND 4.0 International license.

278 mutant embryos, 5EU punctae are also readily detected outside of RAB-7 vesicles, and
279 there does not appear to be significantly more 5EU retained within RAB-7 vesicles (Fig.
280 6*A*, lower row). Thus, although silencing by inherited dsRNA involves early steps in the
281 endocytotic pathway, the dsRNA appears to transit this system rapidly. Although *sid-1* is
282 required for inherited silencing, its activity is not apparent in the localization of 5EU-
283 labeled dsRNA in oocytes or early embryos.
284

285 Discussion

286 Intercellular dsRNA transport in *C. elegans* via the dsRNA channel SID-1 supports
287 systemic gene silencing throughout the animal and its progeny. Here, we have
288 described and characterized the maternal and embryonic processes that support
289 intergenerational dsRNA transport, as summarized in figure 6*B*.
290 First, we more fully described the result of dsRNA injection into the gonad. In
291 wild-type animals, dsRNA injection into a single gonad arm results in robust silencing in
292 nearly all progeny, while similar injection in *sid-1* mutant results in transitory silencing
293 and only in progeny derived from the injected gonad arm (Figure 1; (WINSTON 2002;
294 WINSTON *et al.* 2002). While we still do not understand how injected dsRNA escapes
295 the injected gonad arm or its long-term persistence within the injected animals, its
296 subsequent uptake into both gonad arms can occur by either a *sid-1*-dependent process
297 or a *sid-1*-independent but *rme-2*-dependent process (Figure 2). Consistent with the
298 role of RME-2 as an endocytosis receptor, *sid-1* activity is required subsequently,
299 presumably to release dsRNA from a membrane enclosed compartment (Figure 3). A
300 recent report concluded that silencing in progeny in response to ingested dsRNA is
301 dependent on *rme-2* (MARRÉ *et al.* 2016). Because this conflicts with our results, we
302 repeated their analysis, discovering that progeny silencing in response to parental
303 feeding RNAi is developmentally restricted, being most effective in adults. We found
304 that the progeny of *rme-2* adults are efficiently silenced by feeding RNAi, and suggest
305 that the slowed development of *rme-2* animals may have compromised their analysis
306 (Figure 3).
307 The redundancy between *sid-1* and *rme-2* for uptake and transport of dsRNAs
308 into the germline is contrasted by the necessity for both *sid-1* and *sid-2* for uptake and
309 transport of dsRNAs into the intestine (WINSTON *et al.* 2007). Presumably, oocyte
310 expressed SID-1 localizes to the plasma membrane adjacent to the PC space, whereas
311 intestinal expressed SID-1 does not localize the lumenal plasma membrane. This
312 difference may reflect the privileged environment of the PC space, relative to the
313 ingested intestinal milieu. An alternative but unlikely scenario is that a second oocyte
314 expressed endocytosis receptor accounts for the *rme-2*-independent uptake. However
315 such activity should be apparent in silencing the progeny of *rme-2; sid-1* double mutants,
316 which is not detected. The redundancy between *sid-1* and *rme-2* is significant in light of
317 reports of *sid-1*-independent RNAi-dependent transgenerational inheritance (SCHOTT *et*
318 *al.* 2014). It will be interesting to determine whether alternative RNA uptake
319 mechanisms mediate transgenerational inheritance and inheritance of acquired traits.
320 Our genetic and cytological analysis of dsRNA in oocytes and embryos revealed
321 a role for *sid-5* alongside *sid-1* in dsRNA import and showed that despite sharing an
322 endocytosis receptor, yolk protein and dsRNA travel independent intracellular routes.
323 SID-5 is a late endosomal/multivesicular body localized protein required for efficient

bioRxiv preprint doi: https://doi.org/10.1101/156232; this version posted June 26, 2017. The copyright holder for this preprint (which was not certified by peer review) is the author/funder, who has granted bioRxiv a license to display the preprint in perpetuity. It is made available under aCC-BY-NC-ND 4.0 International license.

324 systemic RNAi (HINAS *et al.* 2012). Tissue-specific rescue experiments showed that *sid-*
325 *5* expression in the intestine but not the muscle was sufficient for RNAi silencing of a
326 muscle gene (HINAS *et al.* 2012). The results presented here, showing a role for SID-5 in
327 dsRNA import, suggest that efficient release of endocytosed ingested dsRNA to the
328 cytoplasm is important for subsequent export to muscle cells. Our cytological analysis
329 of dsRNA within oocytes and embryos indicates that yolk and dsRNA rarely co-localize
330 (Figure 5). This result challenges the assumption that dsRNA enters ooctyes with yolk
331 granules. Furthermore, the observation that EU- but not Cy5-labeled dsRNA injected
332 into the PC is internalized within oocytes (Figure 4) suggest specificity in dsRNA uptake
333 rather than proposed non-specific mechanisms (MARRÉ *et al.* 2016). While *sid-1* and
334 *sid-5* are required for this endocytosed dsRNA to trigger RNAi silencing, *sid-1* activity is
335 apparently not required for transit to post-RAB-7 compartments (Figure 5).
336 Our results support a model where SID-1 is required to facilitate dsRNA transport
337 into the cytoplasm directly from extracellular spaces as well as from endocytotic
338 vesicles. Indeed, other organisms capable of systemic RNAi may be more reliant on
339 endocytosis of dsRNA, including organisms that lack SID-1 (SALEH *et al.* 2006), and at
340 least one insect species has been shown to use both SID-1 and endocytosis (CAPPELLE
341 *et al.* 2016). A better understanding of the mechanisms by which circulating RNA
342 reaches the next generation will help us identify endogenous inherited RNAs.
343
344 ## Materials and Methods
345 ### Strains
346 The following strains were used: N2 wild-type, HC977 *sid-1(qt101)*, HC970 *sid-1(qt78)*,
347 *sid-1(qt78)*; *sid-2(qt40)*, HC306 *sid-2(qt40)*, HC770 *sid-3(tm342)*, HC302 *sid-5(qt24)*,
348 HC975 *sid-1(qt78)*; *sid-3(tm342)*, HC976 *sid-1(qt78)*; *sid-5(qt24)*, DH1390 *rme-2(b1008)*,
349 HC1064 *rme-2(b1008)*; *sid-1(qt101)*, HC17 bIs1[*vit-2::GFP* + *rol-6(su1006)*]; *emb-*
350 *27(g48)*, HC1060 *sid-1(qt101)*; bIs1[*vit-2::GFP* + *rol-6(su1006)*], RT123 pwIs21[*unc-*
351 *119*(+); P*pie-1*::*GFP*::*rab-7*], HC1099 *sid-1(qt78)*; pwIs21[*unc-119*(+); P*pie-1*::*GFP*::*rab-*
352 *7*]
353 ### RNAi
354 Injections of *unc-22* dsRNA were done at a concentration of approximately ~2 mg/ml.
355 For pseudocoelom injections, the needle was inserted beyond the bend of the gonad
356 arm but before the pharynx or else in the tail beyond the gonad. Injections were done at
357 ~13-20 psi, with successful injections appearing to briefly "highlight" tissues along the
358 entire length of the animal under DIC. For RNAi experiments involving a cross, injected
359 animals were recovered together on a single OP50 plate for ~12 h before the addition of
360 triple the number of appropriate males. After ~36 h of mass mating, individual injected
361 hermaphrodites were singled to new plates along with 3 males and allowed to lay eggs
362 for ~48 h before all P_0 animals were removed. For the feeding RNAi timing experiment,
363 a mixed population of N2 animals was bleached in a basic sodium hypochlorite solution
364 until adult bodies had dissolved, and the released embryos were rinsed in M9. Embryos
365 were allowed to hatch in shaking M9 for 10 h, and the hatched L1s were then roughly
366 partitioned and transferred to *unc-22* RNAi food (TIMMONS *et al.* 2001) or OP50 plates
367 as appropriate by pipetting. Each subsequent day, animals were washed off of the
368 plates and washed four times in M9 and then transferred to new appropriate bacteria
369 plates. Gravid adults were washed again, and 30 animals from each group were picked

bioRxiv preprint doi: https://doi.org/10.1101/156232; this version posted June 26, 2017. The copyright holder for this preprint (which was not certified by peer review) is the author/funder, who has granted bioRxiv a license to display the preprint in perpetuity. It is made available under aCC-BY-NC-ND 4.0 International license.

370 to individual OP50 plates for F_1 collection. Adult and L4 feeding assays were similarly
371 washed before F_1 collection, but parents were simply picked from mixed populations.
372 Day 1 adults were prepared by isolating L4 larvae and maintaining for 12 h at 20°C.
373 Scoring for the strong twitching phenotype characteristic of *unc-22* silencing was done
374 in 10 mM levamisole in M9 buffer once the F_1 progeny were young adults.

375 **Labeled dsRNA preparation**

376 5EU and Cy5 labeled RNAs were synthesized using the Ampliscribe T7 Flash
377 Transcription Kit (Epicentre) using a modified version of the manufacturer's protocol to
378 include the substituted nucleotides. Detailed procedures can be found in the
379 supplemental methods.

380 **Immunohistochemistry**

381 Slides for microscopy were prepared as in (HINAS *et al.* 2012), with some modifications
382 for click labeling of 5EU. For mounted adults, 5EU was conjugated to an Alexa 594-
383 azide using the Click-iT RNA Imaging Kit (Invitrogen). For embryos, 5EU was first
384 conjugated to biotin-azide (Lumiprobe) using the same Click-iT kit, followed by the
385 Alexa Fluor 594 Tyramide SuperBoost Kit with streptavidin (Invitrogen) for enhanced
386 signal. Detailed procedures can be found in the supplemental methods.

387 **Microscopy**

388 Most images were captured using a Zeiss LSM880 microscope using the ZEN software
389 (Zeiss) at the Harvard Center for Biological Imaging. Embryo images from Cy5/5EU
390 dual labeling experiments were captured using a Zeiss Axiovert 200 spinning disk
391 confocal microscope with Axiovision (Zeiss).
392
393

bioRxiv preprint doi: https://doi.org/10.1101/156232; this version posted June 26, 2017. The copyright holder for this preprint (which was not certified by peer review) is the author/funder, who has granted bioRxiv a license to display the preprint in perpetuity. It is made available under aCC-BY-NC-ND 4.0 International license.

394 **References**

395 Alcazar, R. M., R. Lin and A. Z. Fire, 2008 Transmission dynamics of heritable silencing
396 induced by double-stranded RNA in Caenorhabditis elegans. Genetics 180**:**
397 1275-1288.
398 Buckley, B. A., K. B. Burkhart, S. G. Gu, G. Spracklin, A. Kershner *et al.*, 2012 A
399 nuclear Argonaute promotes multigenerational epigenetic inheritance and
400 germline immortality. Nature 489**:** 447-451.
401 Cappelle, K., C. F. R. de Oliveira, V. B. Eynde, O. Christiaens and G. Smagghe, 2016
402 The involvement of clathrin-mediated endocytosis and two Sid-1-like
403 transmembrane proteins in double-stranded RNA uptake in the Colorado potato
404 beetle midgut. Insect Molecular Biology 25**:** 315-323.
405 Feinberg, E. H., and C. P. Hunter, 2003 Transport of dsRNA into cells by the
406 transmembrane protein SID-1. Science 301**:** 1545-1547.
407 Feng, Y., B. Press and A. Wandinger-Ness, 1995 Rab 7: an important regulator of late
408 endocytic membrane traffic. The Journal of Cell Biology 131**:** 1435-1452.
409 Fire, A., S. Xu, M. K. Montgomery, S. A. Kostas, S. E. Driver *et al.*, 1998 Potent and
410 specific genetic interference by double-stranded RNA in Caenorhabditis elegans.
411 Nature 391**:** 806-811.
412 Grant, B., and D. Hirsh, 1999 Receptor-mediated endocytosis in the Caenorhabditis
413 elegans oocyte. Molecular biology of the cell 10**:** 4311-4326.
414 Grishok, A., H. Tabara and C. C. Mello, 2000 Genetic requirements for inheritance of
415 RNAi in C. elegans. Science 287**:** 2494-2497.
416 Guang, S., A. F. Bochner, K. B. Burkhart, N. Burton, D. M. Pavelec *et al.*, 2010 Small
417 regulatory RNAs inhibit RNA polymerase II during the elongation phase of
418 transcription. Nature 465**:** 1097-1102.
419 Guang, S., A. F. Bochner, D. M. Pavelec, K. B. Burkhart, S. Harding *et al.*, 2008 An
420 Argonaute transports siRNAs from the cytoplasm to the nucleus. Science 321**:**
421 537-541.
422 Hamilton, A. J., and D. C. Baulcombe, 1999 A species of small antisense RNA in
423 posttranscriptional gene silencing in plants. Science 286**:** 950-952.
424 Hinas, A., A. J. Wright and C. P. Hunter, 2012 SID-5 is an endosome-associated protein
425 required for efficient systemic RNAi in C. elegans. Current biology 22**:** 1938-1943.
426 Hutvágner, G., and P. D. Zamore, 2002 RNAi: nature abhors a double-strand. Current
427 opinion in genetics & development 12**:** 225-232.
428 Ivashuta, S., Y. Zhang, B. E. Wiggins, P. Ramaseshadri, G. C. Segers *et al.*, 2015
429 Environmental RNAi in herbivorous insects. RNA 21**:** 840-850.
430 Jao, C. Y., and A. Salic, 2008 Exploring RNA transcription and turnover in vivo by using
431 click chemistry. Proc Natl Acad Sci USA 105**:** 15779-15784.
432 Jose, A. M., Y. A. Kim, S. Leal-Ekman and C. P. Hunter, 2012 Conserved tyrosine
433 kinase promotes the import of silencing RNA into Caenorhabditis elegans cells.
434 Proc Natl Acad Sci USA 109**:** 14520-14525.
435 Jose, A. M., J. J. Smith and C. P. Hunter, 2009 Export of RNA silencing from C. elegans
436 tissues does not require the RNA channel SID-1. Proceedings of the National
437 Academy of Sciences of the United States of America 106**:** 2283-2288.

bioRxiv preprint doi: https://doi.org/10.1101/156232; this version posted June 26, 2017. The copyright holder for this preprint (which was not certified by peer review) is the author/funder, who has granted bioRxiv a license to display the preprint in perpetuity. It is made available under aCC-BY-NC-ND 4.0 International license.

438 Marré, J., E. C. Traver and A. M. Jose, 2016 Extracellular RNA is transported from one
439 generation to the next in Caenorhabditis elegans. Proc Natl Acad Sci USA 113:
440 12496-12501.
441 McEwan, D. L., A. S. Weisman and C. P. Hunter, 2012 Uptake of extracellular double-
442 stranded RNA by SID-2. Molecular Cell 47: 746-754.
443 Saleh, M.-C. C., R. P. van Rij, A. Hekele, A. Gillis, E. Foley *et al.*, 2006 The endocytic
444 pathway mediates cell entry of dsRNA to induce RNAi silencing. Nature Cell
445 Biology 8: 793-802.
446 Schott, D., I. Yanai and C. P. Hunter, 2014 Natural RNA interference directs a heritable
447 response to the environment. Scientific Reports 4: 7387.
448 Sharp, P. A., 2001 RNA interference—2001. Genes & development 15: 485-490.
449 Sharrock, W. J., M. E. Sutherlin, K. Leske, T. K. Cheng and T. Y. Kim, 1990 Two distinct
450 yolk lipoprotein complexes from Caenorhabditis elegans. The Journal of
451 biological chemistry 265: 14422-14431.
452 Shih, J. D., and C. P. Hunter, 2011 SID-1 is a dsRNA-selective dsRNA-gated channel.
453 RNA 17: 1057-1065.
454 Timmons, L., D. L. Court and A. Fire, 2001 Ingestion of bacterially expressed dsRNAs
455 can produce specific and potent genetic interference in Caenorhabditis elegans.
456 Gene 263: 103-112.
457 Winston, W. M., 2002 Systemic RNAi Defective Mutants in the Nematode *C. elegans*.
458 Harvard University.
459 Winston, W. M., C. Molodowitch and C. P. Hunter, 2002 Systemic RNAi in C. elegans
460 requires the putative transmembrane protein SID-1. Science 295: 2456-2459.
461 Winston, W. M., M. Sutherlin, A. J. Wright, E. H. Feinberg and C. P. Hunter, 2007
462 Caenorhabditis elegans SID-2 is required for environmental RNA interference.
463 Proc Natl Acad Sci USA 104: 10565-10570.
464 Zamore, P. D., T. Tuschl, P. A. Sharp and D. P. Bartel, 2000 RNAi: double-stranded
465 RNA directs the ATP-dependent cleavage of mRNA at 21 to 23 nucleotide
466 intervals. Cell 101: 25-33.
467

bioRxiv preprint doi: https://doi.org/10.1101/156232; this version posted June 26, 2017. The copyright holder for this preprint (which was not certified by peer review) is the author/funder, who has granted bioRxiv a license to display the preprint in perpetuity. It is made available under aCC-BY-NC-ND 4.0 International license.

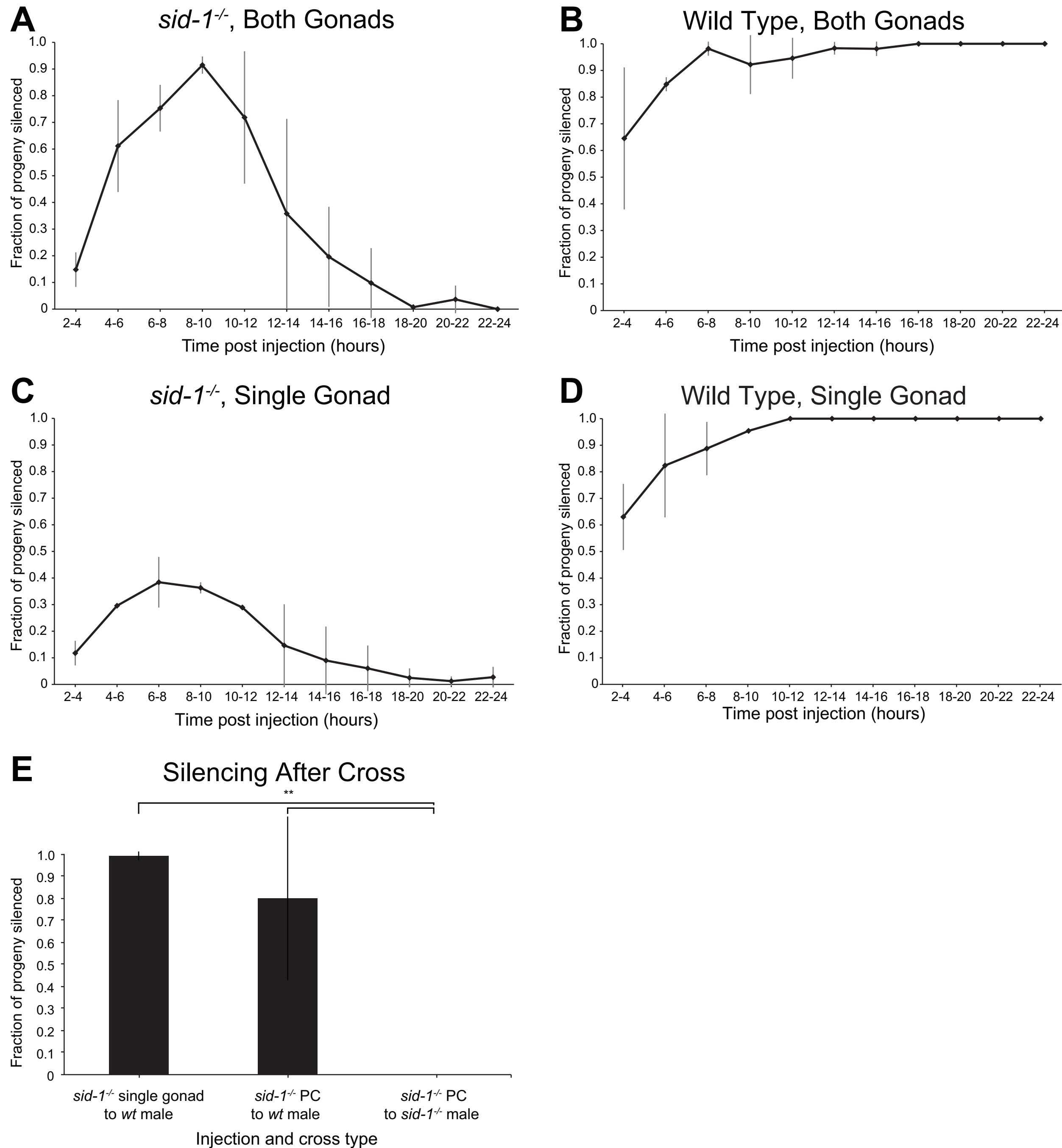

468
469 **Fig. 1.** *sid-1*-dependent and -independent silencing in progeny of dsRNA injected
470 parents. (*A-D*) Time course of fraction of progeny with the Unc-22 phenotype laid after
471 *unc-22* dsRNA gonad injection into wild-type or *sid-1* mutant hermaphrodites. (*E*)
472 Fraction of progeny with Unc-22 phenotype following *unc-22* dsRNA gonad or PC
473 injection into *sid-1*$^{-/-}$ mutant hermaphrodites crossed to wild-type or *sid-1* mutant males.
474 Error bars in (*A-D*) represent standard error from two experiments with 10 injected
475 hermaphrodites each. Error bars in (*E*) represent standard deviation from 4, 6, and 3
476 injected hermaphrodites, left to right. $^{**}p < 0.01$ by Welch's *t* test.
477

bioRxiv preprint doi: https://doi.org/10.1101/156232; this version posted June 26, 2017. The copyright holder for this preprint (which was not certified by peer review) is the author/funder, who has granted bioRxiv a license to display the preprint in perpetuity. It is made available under aCC-BY-NC-ND 4.0 International license.

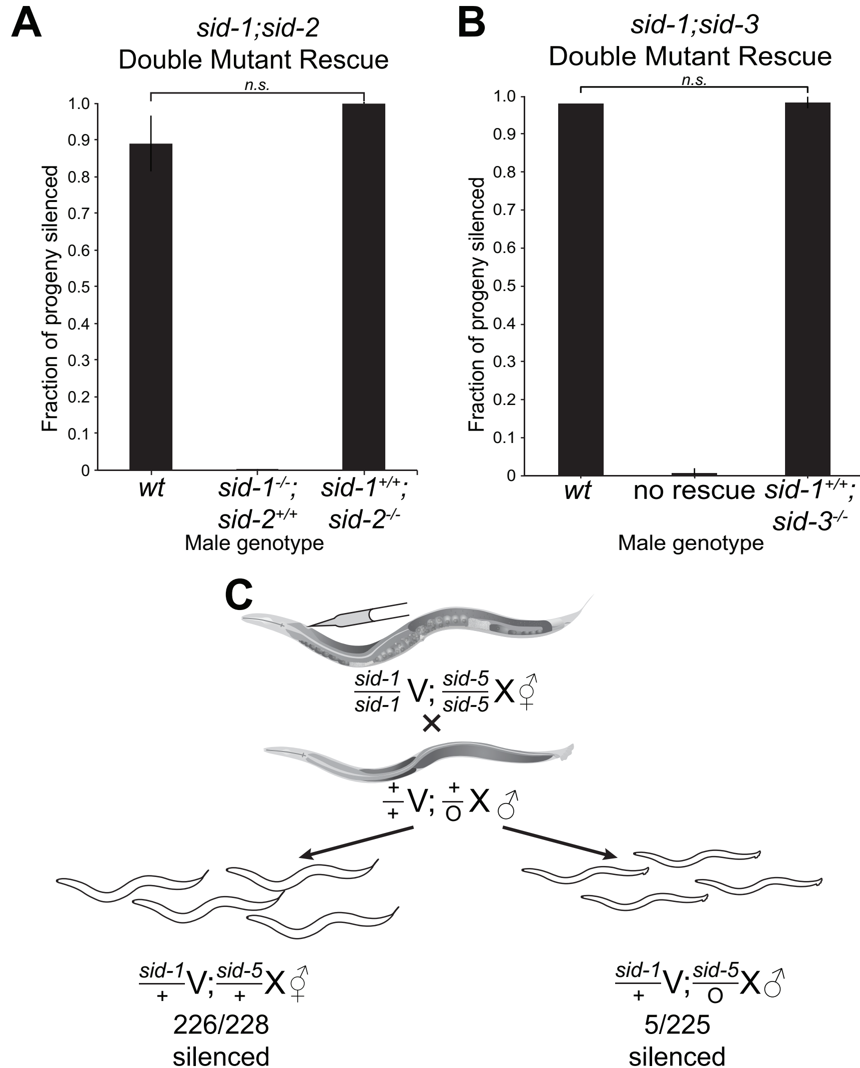

478
479 **Fig. 2.** Maternal and zygotic Sid-dependence of inherited silencing. (*A*) Fraction of *unc-*
480 *22* silenced cross progeny from *sid-1; sid-2* double-mutant hermaphrodites first PC-
481 injected with *unc-22* dsRNA and then crossed to either wild-type, *sid-1; sid-2* double
482 mutant, or *sid-2* single mutant males. (*B*) Fraction of *unc-22* silenced cross progeny
483 from *sid-1; sid-3* double-mutant hermaphrodites first PC-injected with *unc-22* dsRNA
484 and then crossed to wild-type, *sid-1; sid-3* double mutant, or *sid-3* single mutant males.
485 (*C*) Schematic of the injection, cross, and *unc-22* silencing scoring of cross progeny
486 from *sid-1; sid-5* double mutant hermaphrodites first PC-injected with *unc-22* dsRNA
487 and then crossed to wild-type males. *sid-5* is X-linked, thus hermaphrodite progeny are
488 heterozygous and males are hemizygous. Error bars in (*A, B*) represent standard
489 deviation from 4, 7, and 5 injected hermaphrodites in (*A*) and 1, 3, and 3 injected
490 hermaphrodites in (*B*). 3 injected hermaphrodites in (*C*). *n.s.* = not significant.
491

bioRxiv preprint doi: https://doi.org/10.1101/156232; this version posted June 26, 2017. The copyright holder for this preprint (which was not certified by peer review) is the author/funder, who has granted bioRxiv a license to display the preprint in perpetuity. It is made available under aCC-BY-NC-ND 4.0 International license.

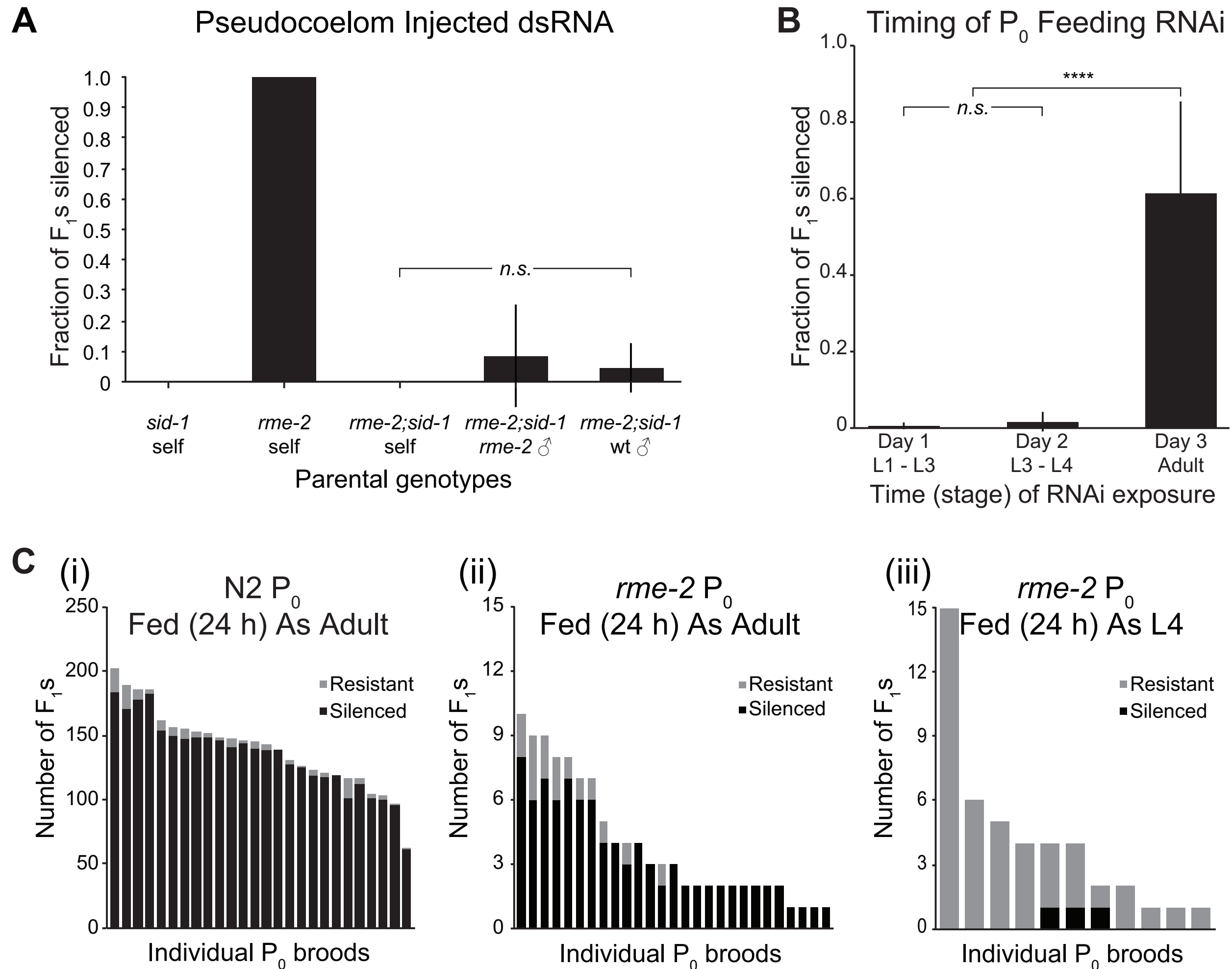

492
493 **Fig. 3.** Maternal RME-2-dependent inherited silencing. (*A*) Fraction of progeny sensitive
494 to *unc-22* silencing among the self-progeny or indicated cross-progeny of
495 hermaphrodites PC-injected with *unc*-22 dsRNA. *n* = 6, 5, 3, 4, and 12 injected
496 hermaphrodites respectively. (*B*) Fraction of progeny sensitive to *unc-22* silencing after
497 wild-type parents were exposed to feeding RNAi at the given periods of time after
498 hatching. *n* = 30 treated parents for each group. (*C*) Sensitivity to *unc-22* feeding RNAi
499 in progeny after treating (*i*) wild-type parents as adults, (*ii*) *rme-2* mutant parents as
500 adults, or (*iii*) *rme-2* mutant parents as L4 larvae. Because *rme-2* mutants have severely
501 reduced fecundity, the results from each individual parent are presented separately for
502 clarity, with silenced progeny represented in black bars and non-silenced progeny in
503 grey bars. All error bars represent standard deviation. ****$p < 0.00001$ by *t* test. *n.s.* =
504 not significant.
505

bioRxiv preprint doi: https://doi.org/10.1101/156232; this version posted June 26, 2017. The copyright holder for this preprint (which was not certified by peer review) is the author/funder, who has granted bioRxiv a license to display the preprint in perpetuity. It is made available under aCC-BY-NC-ND 4.0 International license.

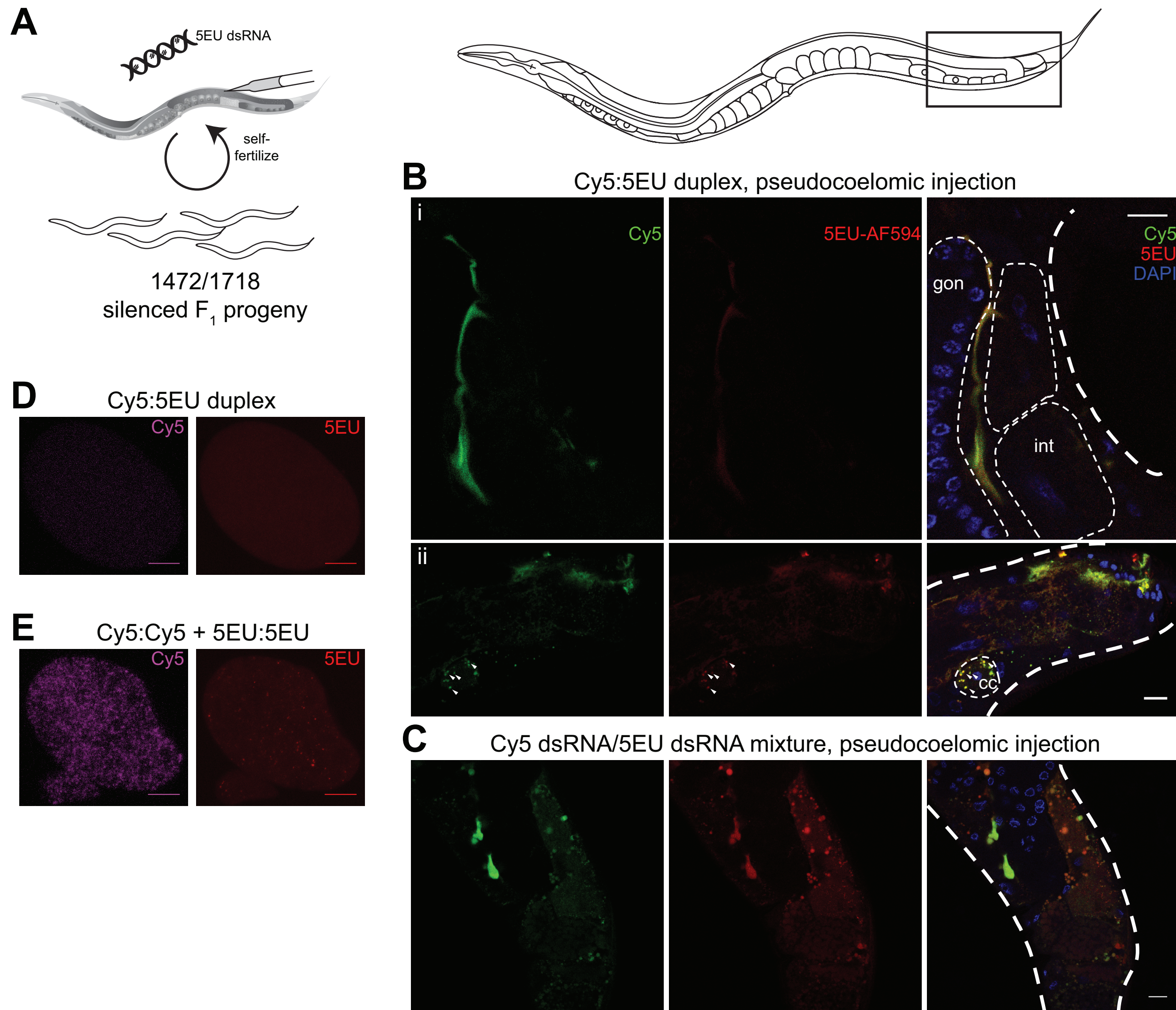

506
507 **Fig. 4.** Visualizing 5-Ethynyluridine (5EU) labeled functional dsRNA. (*A*) Injected 5EU
508 dsRNA injected into only one gonad arm produces >50% affected progeny. *n* = 8
509 injected hermaphrodites. (*B*) Localization of PC injected Cy5::5EU heteroduplex dsRNA.
510 Cy5 fluorescence and 5EU detection co-localize in the pseudocoelom (*i*) and a
511 coelomocyte (*cc)* (ii; white arroweads). (*C*) Independent localization of PC injected 5EU
512 and Cy5 labeled dsRNA. Images in (*B*) and (*C*) represent portions of dissected and
513 partially flattened adult hermaphrodites. Thick dotted lines mark the boundary of the
514 animal, and thinner dotted lines mark structures such as the gonad (*gon*) or intestinal
515 cells (*int*) as landmarks for orientation. (*D, E*) Cy5 and 5EU signal in embryos collected
516 from adults injected with the dsRNA species described in (*B*) and (*C*) respectively. The
517 two Cy5 images are overexposed, revealing diffuse autofluorescence and no detectable
518 RNA. Scale bars = 10 μm.
519

bioRxiv preprint doi: https://doi.org/10.1101/156232; this version posted June 26, 2017. The copyright holder for this preprint (which was not certified by peer review) is the author/funder, who has granted bioRxiv a license to display the preprint in perpetuity. It is made available under aCC-BY-NC-ND 4.0 International license.

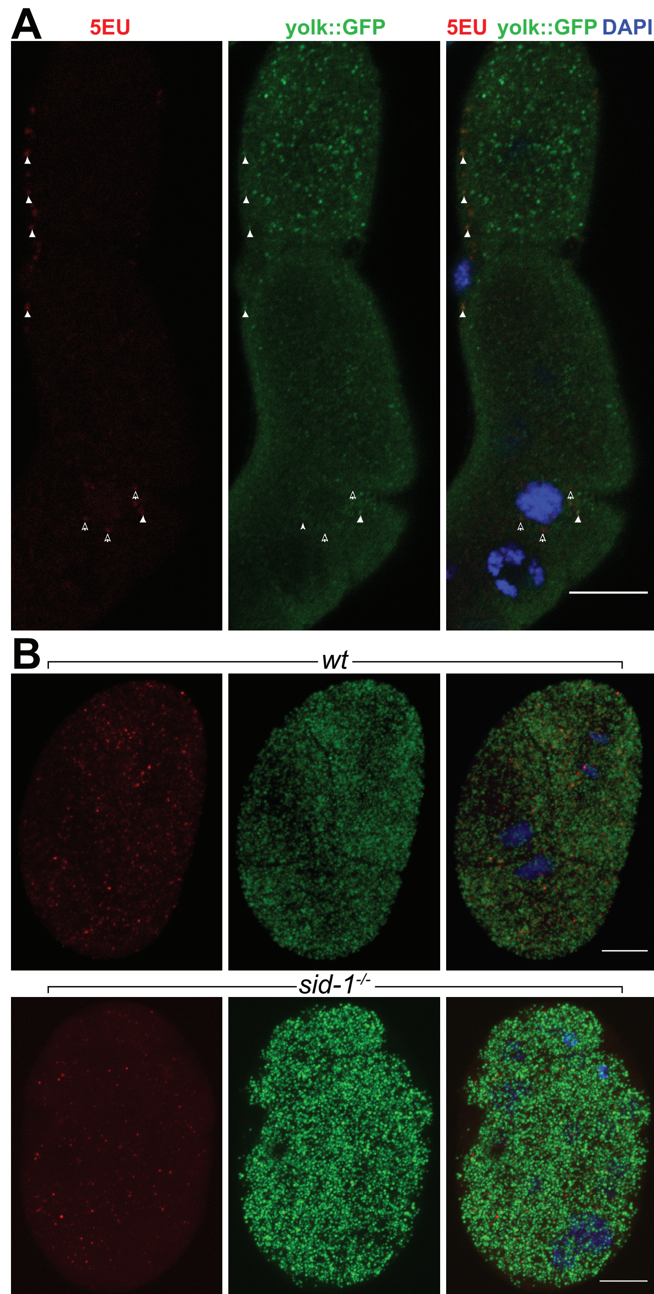

520
521 **Fig. 5.** Co-localization of 5EU-labeled dsRNA and VIT-2::GFP on and within oocytes.
522 (*A*) PC-injected 5EU-labeled dsRNA co-localized with GFP-labeled yolk at the surface
523 of developing oocytes (white arrowheads), but not intracellularly (notched arrowheads).
524 More proximal oocyte (top) contains more VIT-2::GFP. (*B*) Maximum *z*-projections of
525 VIT-2::GFP and 5EU-labeled dsRNA in wild-type and *sid-1*$^{-/-}$ embryos show little co-
526 localization. Scale bars = 10 μm.
527

bioRxiv preprint doi: https://doi.org/10.1101/156232; this version posted June 26, 2017. The copyright holder for this preprint (which was not certified by peer review) is the author/funder, who has granted bioRxiv a license to display the preprint in perpetuity. It is made available under aCC-BY-NC-ND 4.0 International license.

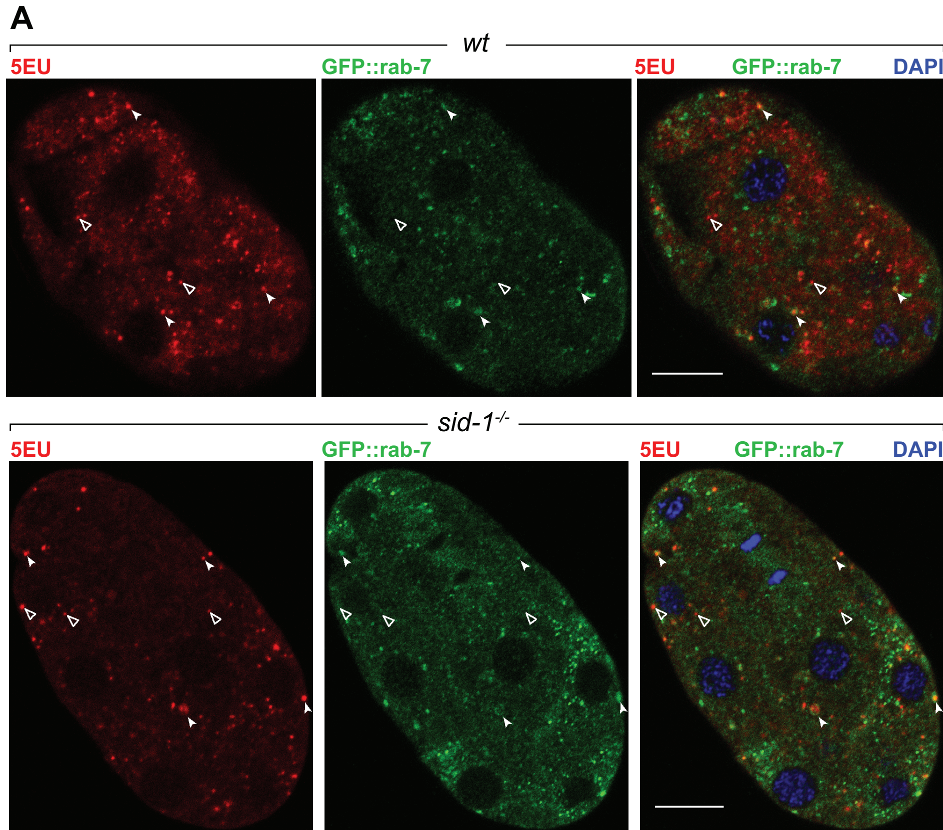

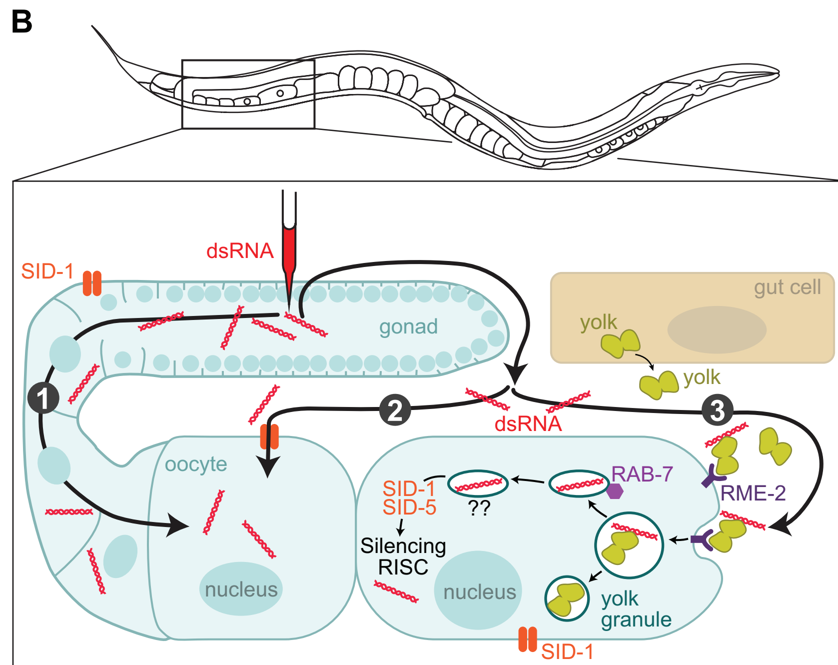

528
529 **Fig. 6.** Co-localization of dsRNA and GFP::RAB-7. (*A*) 5EU foci detected in embryos
530 after pseudocoelomic 5EU-labeled dsRNA injection co-localizes with GFP:: RAB-7
531 (notched arrowheads) but is also found outside of RAB-7 structures (open arrowheads)
532 in both wild-type (upper row) and *sid-1* mutant (*Lower row*) embryos. Scale bars = 10
533 μm. (*B*) Model for three inherited dsRNA transport pathways. 1) DsRNA injected directly

bioRxiv preprint doi: https://doi.org/10.1101/156232; this version posted June 26, 2017. The copyright holder for this preprint (which was not certified by peer review) is the author/funder, who has granted bioRxiv a license to display the preprint in perpetuity. It is made available under aCC-BY-NC-ND 4.0 International license.

534 into the syncytial germline can silence the resulting progeny without SID-1. Some
535 injected dsRNA exits the gonad to the PC and is then 2) endocytosed into developing
536 oocytes via LDL receptor super-family member RME-2, or 3) this PC dsRNA can also
537 be directly transported into oocytes via SID-1.

bioRxiv preprint doi: https://doi.org/10.1101/156232; this version posted June 26, 2017. The copyright holder for this preprint (which was not certified by peer review) is the author/funder, who has granted bioRxiv a license to display the preprint in perpetuity. It is made available under aCC-BY-NC-ND 4.0 International license.

Supplemental methods

Labeled RNA preparation

Purified RNA was synthesized by *in vitro* transcription (IVT) from a DNA template containing T7 promoter sequences. For labeled and unlabeled *unc-22* dsRNA, template DNA was prepared by PCR using primers with the T7 promoter sequence appended to the 5' end of both forward and reverse primers. For the Cy5- and 5EU-containing RNA in Fig. 4, the forward and reverse strands of the eventual dsRNA were prepared independently from template DNA containing only a single T7 promoter.

IVT was performed using an Ampliscribe T7 Flash kit (Epicentre) according to manufacturer instructions with the following modifications for labeled RNAs. For 5EU-labeled RNA, the 100 mM UTP in the reaction was substituted with an equal volume of a 1:1 mixture of UTP and 100mM 5-ethynyl-UTP (Jena Bioscience). 5EU-labeled RNA can also be synthesized using only 5-ethynyl-UTP and no unmodified UTP and behaves similarly in the experiments we performed. For Cy5-labeled RNA, instead of individually adding 0.9 μl of each NTP, a mixture of equal amounts of 100 mM ATP, CTP, and GTP was prepared, and 4.55 μl of this mixture was added to the reaction, followed by 1 μl of 100 mM UTP and 3 μl of 10 mM Cy5-UTP (Amersham). IVT reactions of labeled RNA were incubated at 37°C for 4.5 h, and then treated with DNase I at 37°C for 15 min. Synthesized RNA was purified using an RNeasy kit (Qiagen). Equal quantities of complementary strands of RNA were then annealed together by heating mixtures to 95°C for 2 min and then gradually lowering the temperature to 20°C at a rate of 0.1°C per second.

bioRxiv preprint doi: https://doi.org/10.1101/156232; this version posted June 26, 2017. The copyright holder for this preprint (which was not certified by peer review) is the author/funder, who has granted bioRxiv a license to display the preprint in perpetuity. It is made available under aCC-BY-NC-ND 4.0 International license.

Immunohistochemistry

After injection of 5EU-labeled RNA, adults or isolated embryos were transferred to a poly-L-lysine coated slide and covered with 10 μl of 4% paraformaldehyde solution (PFA). A square cover glass was then placed on to the sample, and excess liquid removed by wicking to a tissue paper until the point of mechanical rupturing of eggshells or cuticles to provide access to the fixative. Samples were then left to fix for 15 min at room temperature before flash freezing in liquid nitrogen. Afterwards, the cover glass was removed with a razor blade to help remove cuticles and eggshells. Samples were then fixed in -20°C methanol for 15 min, and then briefly rinsed in PBS. The final preparation step before labeling was sample permeabilization in a 0.1% Tween-20 in phosphate buffered saline (PBS) solution for 15 min at room temperature.

Labeling of samples containing 5EU-RNA was performed with a Click-iT RNA Imaging kit (Invitrogen) according to manufacturer instructions, but reaction volumes reduced to 100 μl per slide. For adult worm samples, labeling was done with Alexa Fluor 594 azide (Thermo Fisher), but embryo samples typically substituted 2.66 μM biotin azide (Lumiprobe) for additional signal amplification. Click labeling reactions were incubated at room temperature for 30 min and then stopped with addition of stop solution from the kit, and then washed 3 times in PBS. Samples to be labeled only with Alexa fluor could be mounted in Vectashield with DAPI and sealed under a coverslip at this point, or further processed with additional labeling.

Embryo samples requiring signal amplification were further processed with the Alexa Fluor 594 Tyramide SuperBoost Kit with streptavidin (Invitrogen) according to manufacturer instructions, with the tyramide labeling reaction allowed to proceed for 8

bioRxiv preprint doi: https://doi.org/10.1101/156232; this version posted June 26, 2017. The copyright holder for this preprint (which was not certified by peer review) is the author/funder, who has granted bioRxiv a license to display the preprint in perpetuity. It is made available under aCC-BY-NC-ND 4.0 International license.

minutes. After washing 3 times in PBS for 10 minutes each, slides were mounted and sealed, or additionally labeled by antibody staining.

Samples requiring antibody labeling were incubated at room temperature for 1 h with a rabbit polyclonal GFP antibody (Invitrogen) diluted 1:200 in a solution of 5% bovine serum albumin (BSA) in PBS with 0.1% Tween-20. After washing 3 times in PBS, samples were then incubated at room temperature for 1 h with an Alexa Fluor 488-conjugated goat anti-rabbit secondary antibody (Invitrogen). After washing 3 times in PBS, slides were mounted with Vectashield with DAPI and sealed.

bioRxiv preprint doi: https://doi.org/10.1101/156232; this version posted June 26, 2017. The copyright holder for this preprint (which was not certified by peer review) is the author/funder, who has granted bioRxiv a license to display the preprint in perpetuity. It is made available under aCC-BY-NC-ND 4.0 International license.

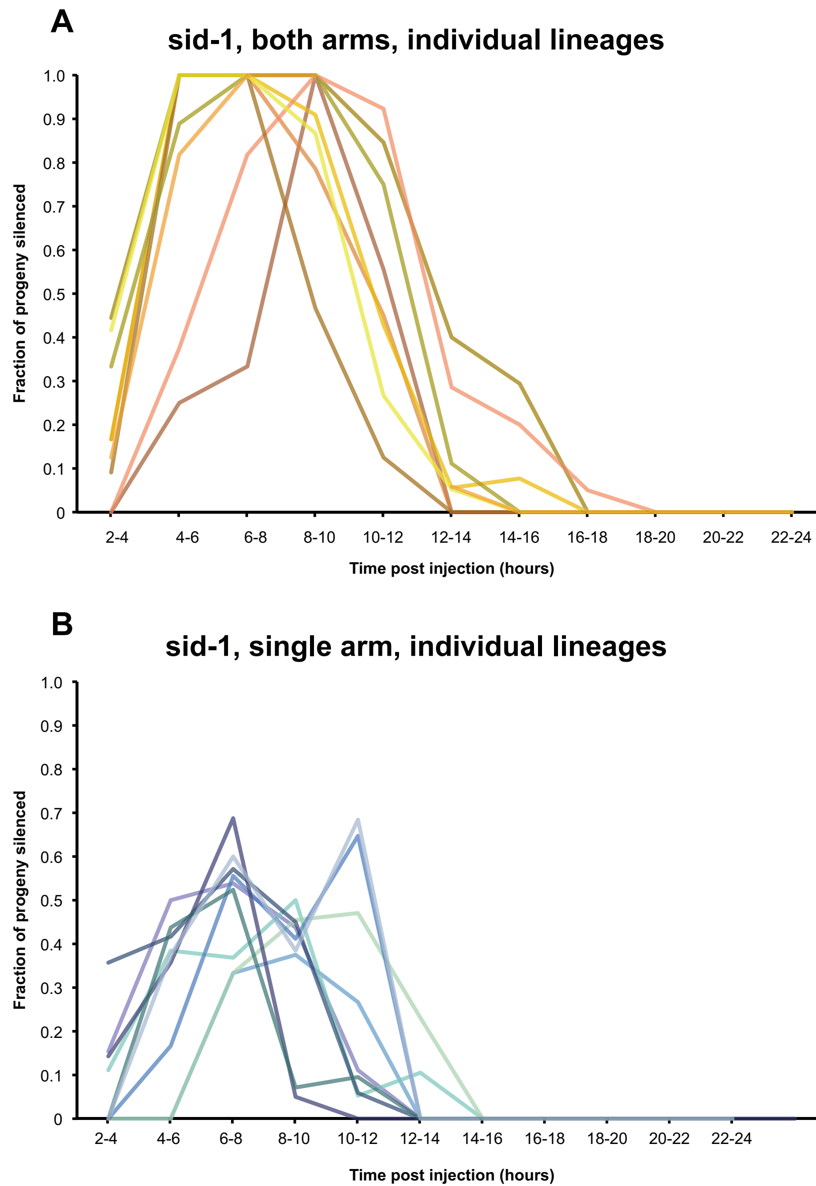

Figure S1. Individual lineages achieve maximum silencing with variable timing

Expanded data from Figure 1, panels 1A and 1C. Each panel in Figure 1 represents the average of two experiments, with the data corresponding to the progeny of each 10 injected animals in each duplicate. Here, the data from one of the replicates from panels 1A and 1C respectively are expanded in (A) and (B) to show the data from each individual injected animal as a separate line.